


# Dephosphorization of High-Phosphorus Oolitic Iron Ore By Prereduction with Carbon Monoxide Followed By Smelting



Bakyt Suleimen<sup>1,2,\*</sup> , Nurlybai Kosdauletov<sup>1,2</sup>  and Galymzhan Adilov<sup>1,2</sup> 

<sup>1</sup>South Ural State University, Research Laboratory "Hydrogen technologies in metallurgy", Lenin Prospekt 76, Chelyabinsk, 454080, Russia

<sup>2</sup>Department of Metallurgy and Mining, K. Zhubanov Aktobe Regional University, Aktobe, 030000, Kazakhstan

## Abstract:

**Introduction:** The study aims to develop an effective method for selective reduction of iron from high-phosphorus oolitic ore, enabling the subsequent separation of low-phosphorus metallic iron and high-phosphorus slag. The approach involves fluxing the ore with calcium oxide (CaO) to stabilize phosphorus and facilitate its removal.

**Methods:** The oolitic iron ore was fluxed with CaO to achieve a basicity of 2.0, then subjected to oxidative roasting at 1200 °C in a Nabertherm muffle furnace to convert iron phosphates into stable calcium phosphates. Solid-phase reduction was performed in a laboratory Tamman furnace at 1000 °C under a CO atmosphere. Final smelting was conducted at 1600 °C in a vertical Nabertherm furnace to achieve liquid-phase separation of metal and slag. X-ray diffraction and micro-X-ray spectral analysis were used for phase characterization.

**Results:** CO selectively reduced iron to metallic form in both fluxed and non-fluxed samples, while phosphorus remained in the oxide phase. In fluxed samples, phosphorus was primarily present as calcium and aluminum phosphates, and iron was fully metallized. In non-fluxed samples, partial iron reduction occurred with residual phosphorus in iron, calcium, and aluminum phosphates. Upon smelting, non-fluxed ore formed a single melt with 0.1 wt.% phosphorus, whereas fluxed samples yielded separate metal and slag phases, with 0.3 wt.% phosphorus retained in the slag.

**Discussion:** The results confirm that fluxing promotes the formation of stable calcium phosphates, preventing phosphorus reduction and enabling efficient Fe-P separation. The selective reduction of iron by CO was kinetically controlled and did not reduce phosphorus compounds. Compared to non-fluxed treatment, fluxing significantly improves the separation of phosphorus into slag during smelting.

**Conclusion:** This study demonstrates a two-stage process for effective dephosphorization of high-phosphorus oolitic iron ores. Key contributions include the identification of phosphorus stabilization mechanisms via CaO fluxing, successful selective reduction of iron by CO, and development of a method for producing low-phosphorous metal and high-phosphorous slag. The approach offers a promising route for processing refractory iron ores.

**Keywords:** Dephosphorization, oolitic iron ore, iron, phosphorus, solid-phase reduction, carbon monoxide, liquid-phase separation, flux.

© 2025 The Author(s). Published by Bentham Open.

This is an open access article distributed under the terms of the Creative Commons Attribution 4.0 International Public License (CC-BY 4.0), a copy of which is available at: <https://creativecommons.org/licenses/by/4.0/legalcode>. This license permits unrestricted use, distribution, and reproduction in any medium, provided the original author and source are credited.

\*Address correspondence to this author at the South Ural State University, Research Laboratory "Hydrogen technologies in metallurgy", Lenin Prospekt 76, Chelyabinsk, 454080, Russia; E-mail: [bakysuleimen@mail.ru](mailto:bakysuleimen@mail.ru)

Cite as: Suleimen B, Kosdauletov N, Adilov G. Dephosphorization of High-Phosphorus Oolitic Iron Ore By Prereduction with Carbon Monoxide Followed By Smelting. Open Chem Eng J, 2025; 19: e18741231409126. <http://dx.doi.org/10.2174/0118741231409126250731100924>



Received: May 05, 2025  
Revised: June 04, 2025  
Accepted: June 27, 2025  
Published: August 04, 2025



Send Orders for Reprints to  
[reprints@benthamscience.net](mailto:reprints@benthamscience.net)



However, the results of the micro-X-ray spectral analysis of metal and slag samples show that the liquid-phase separation of metallization products obtained in a CO atmosphere results in the conversion of phosphorus into metal, despite that phosphorus was not detected in the metal of metallized samples. We believe that phosphorus is converted into metal due to the extraction of phosphorus by metallic iron at the experimental temperature.

The purpose of this paper is the selective reduction of iron in high-phosphorus oolitic ores with subsequent pyrometallurgical separation into low-phosphorus metal and high-phosphorus slag.

## 2. RESEARCH METHODOLOGY

The base oolitic iron ore of the Ayat deposit, with a  $\text{CaO}/\text{SiO}_2$  basicity of 0.2, was first ground to a fine powder of less than 0.4 mm in size. The ground ore and CaO were simultaneously mixed to bring the  $\text{CaO}/\text{SiO}_2$  basicity to 2.0. The resulting furnace batch was roasted in a Nabertherm muffle furnace in an air atmosphere at 1200 °C and held for an hour. The X-ray phase analysis of the base ore was performed without and with the addition of lime after roasting in an air atmosphere.

The solid-phase reduction experiment was conducted similarly to the previous experiments [10, 11] in a closed Tamman furnace with a graphite heater, which ensured the reducing atmosphere in the furnace volume. The equilibrium composition of the gas phase at 1000 K and 1 atm in the working space of the furnace with a graphite heater consists of 28.06% CO, 4.03%  $\text{CO}_2$ , and 67.91%  $\text{N}_2$ . As the temperature increases, the CO content rises and reaches 34.58% at 1273 K, while the  $\text{CO}_2$  and  $\text{N}_2$  contents decrease to 0.07% and 65.35%, respectively [27]. Two corundum crucibles with samples were installed in the working space of the resistance furnace (Fig. 2). Oolitic ore roasted with the addition of lime was placed in the first crucible, and oolitic ore roasted without the addition of lime was placed in the second crucible. Both crucibles were placed side by side in the furnace with the graphite heater, the furnace was closed with a lid, and the crucibles were heated to 1000 °C and held for three hours. Heating to 1000 °C was carried out over 1.5 hours, corresponding to an average heating rate of approximately 11 °C/min.

The temperature and holding time were selected based on the conditions of the previous experiments on the solid-phase selective reduction of iron. After holding, the furnace was switched off, and the samples were cooled together with the furnace to room temperature. Some samples were filled with epoxy resin and subjected to micro-X-ray spectral and X-ray structural phase analysis; others were subjected to liquid-phase separation.

A vertical resistance furnace was used for the liquid-phase separation of the metallization products. The furnace was preheated to 1600 °C. A corundum crucible with the pre-metallized samples was placed in the heated

furnace. Then, the material was heated and smelted. The smelt was thoroughly mixed, held for five minutes, and then poured onto a metal plate for crystallization. The composition of the resulting metal and slag was studied by micro-X-ray spectral analysis on JOEL's JSM-6460LV scanning electron microscope fitted with an energy-dispersive analyzer manufactured by Oxford Instruments. According to the equipment specifications and standard practice, the typical measurement error for major elements in EDS analysis is  $\pm 0.3$  wt.%.

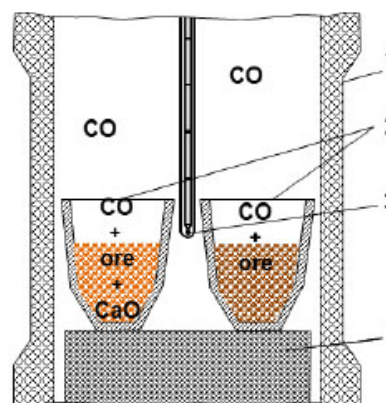


**Fig. (2).** Layout of the working area of the Tamman furnace.

- 1 - graphite heater;
- 2 - crucibles with samples;
- 3 - thermocouple;
- 4 - graphite stand.

## 3. RESULTS AND DISCUSSIONS

Based on the obtained data, we constructed a graph of changes in the mass of oolitic ore at 1200 °C and a holding time of one hour (Fig. 3). Four characteristic sections can be distinguished in the graph of changes in mass from temperature: from 0 to 200 °C, from 200 °C to 400 °C, from 400 to 600 °C, and 600 to 1200 °C. The total loss of ore mass during roasting was 23.8%, with the maximum mass loss in the temperature range of 200–600 °C.

According to the results of X-ray phase analysis, when the base ore is roasted without the addition of CaO in an air atmosphere, goethite  $\text{FeO}(\text{OH})$  loses water and turns into hematite  $\text{Fe}_2\text{O}_3$ , while calcium and magnesium carbonates decompose. Phosphorus in the roasting product is present in the form of  $\text{Ca}_3(\text{PO}_4)_2$ ,  $\text{FePO}_4$ , and  $\text{AlPO}_4$  compounds. After the calcination of the mixture consisting of crushed ore (0.4 mm) and lime in an amount that ensures the basicity of the smelting slag equal to 2,  $\text{FePO}_4$  dissociates with the formation of  $\text{Ca}_4\text{P}_2\text{O}_9$  and  $\text{Ca}_2\text{P}_2\text{O}_7$  compounds (Fig. 4).

A study of the polished sections of ores roasted with carbon monoxide revealed the formation of a metallic iron phase, both on the surface and inside the ore particles (Fig. 5).

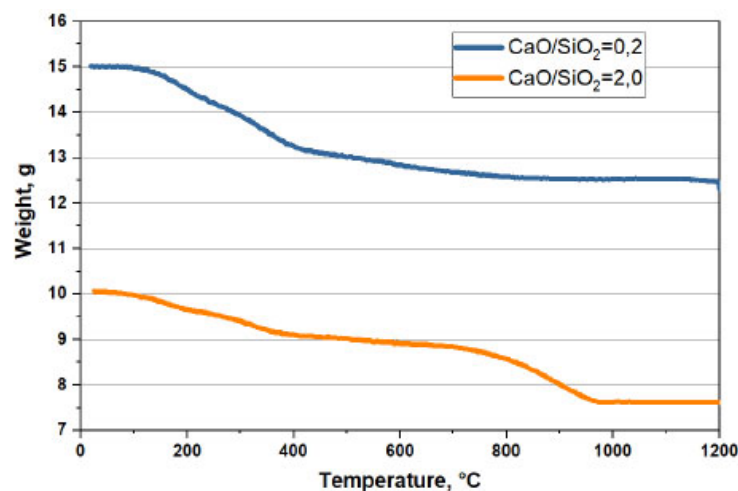


**Fig. (3).** Change in the mass of the base ore without (—) and with (—) CaO during roasting in an air atmosphere.

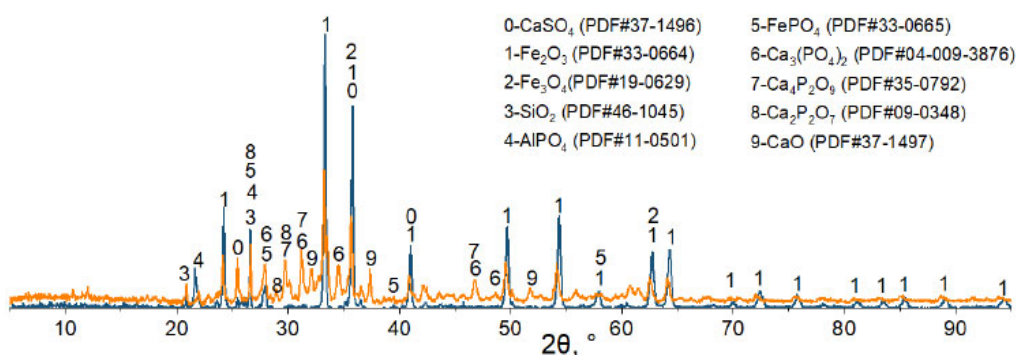


**Fig. (4).** Diffraction patterns of oolitic ore samples without (—) and with (—) CaO after roasting in an air atmosphere.

The boundary between the small metallic particles of iron and the large fragments of dead rock is clearly visible in the non-fluxed samples (Fig. 5a). The reduction of fluxed ores containing CaO led to the formation of larger metallic and fine oxide phases (Fig. 5b). The results of the point scanning in spectra 1 and 3 do not show any signs of phosphorus in metallic iron. This indicates that phosphorus is not reduced by carbon monoxide and remains in the oxide phase, as can be seen in spectra 2 and 4. The residual iron content in the samples with the addition of lime is significantly lower than in the lime-free samples (4.3 at. % and 46.1 at. %, respectively (see Table 2, spectra 4 and 2, respectively)).

Fig. (6) shows the results of the XRD of the samples after reduction roasting. As a result of reduction with carbon monoxide, phosphorus in fluxed roasted ore is contained in the form of aluminum and calcium phosphate, and iron is mainly reduced to metal. In the lime-free ore, iron is partially reduced to metal or present in the form of magnetite and fayalite, and phosphorus is contained in the

form of iron phosphate. The addition of lime increases the degree of iron reduction and leads to the formation of stronger calcium phosphides.

During the liquid-phase separation of metallized samples with lime-free pre-roasting, individual metal 'beads' were not formed, but a whole smelt consisting of a slag phase was obtained. A temperature of 1600°C was apparently relatively low for liquid-phase separation. Fig. (7) shows the structure of the obtained smelt. We can see that the metal did not separate from the slag in this smelt and is present in the slag as individual phases (white spots).

Based on the results of the micro-X-ray spectral analysis, the metal phase in the smelt contains 99.9% iron and 0.1 wt.% phosphorus (Table 3, spectrum 1). The slag consists mainly of aluminum, silicon, and iron oxides. The content of iron in the slag varies from 33.6% to 56.8% (Table 3, spectrum 2, 3), since it was present in the form of fayalite in the metallized sample.



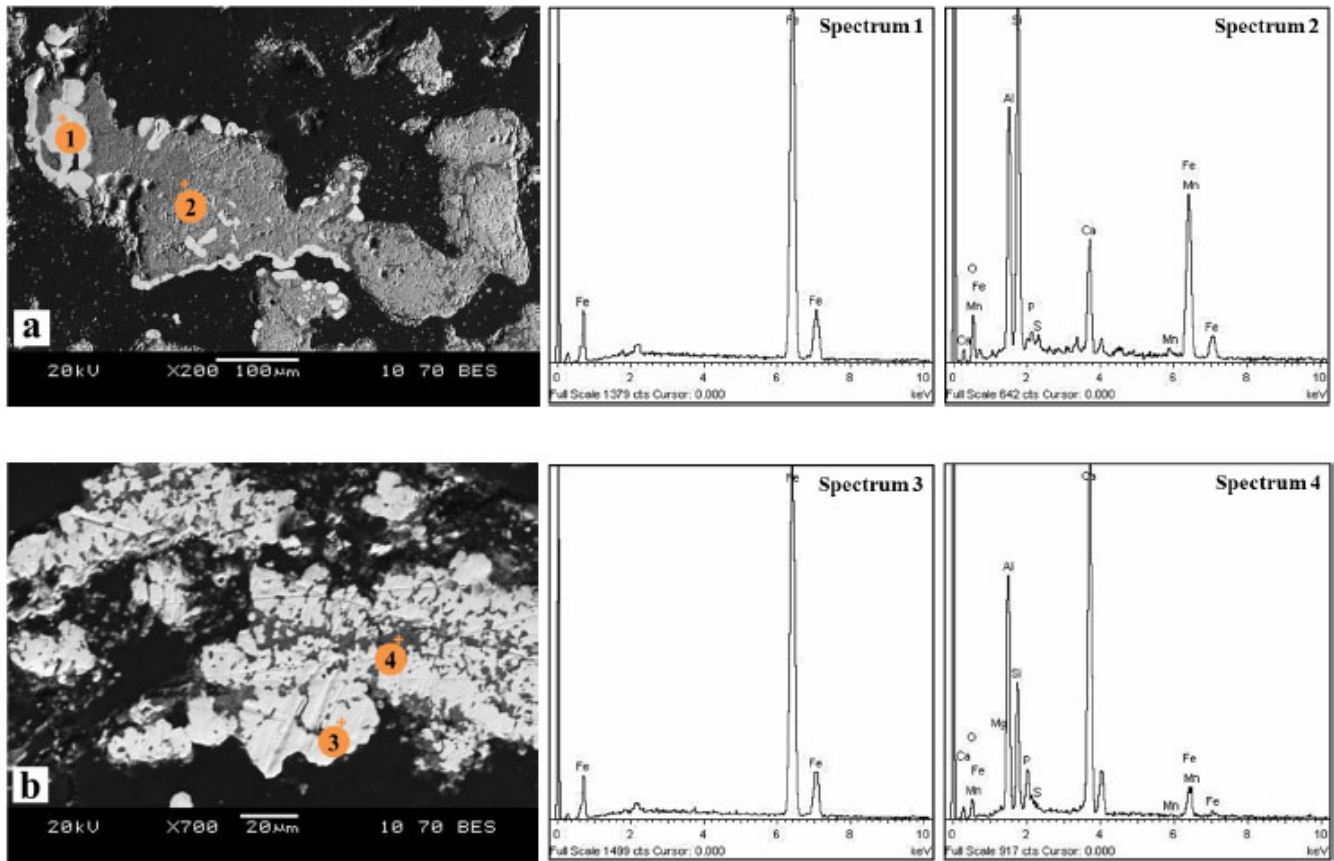


**Fig. (5).** Metallic and oxide particles in ore samples without (a) and with (b) the addition of CaO after reduction roasting with carbon monoxide at 1000°C and a holding time of three hours

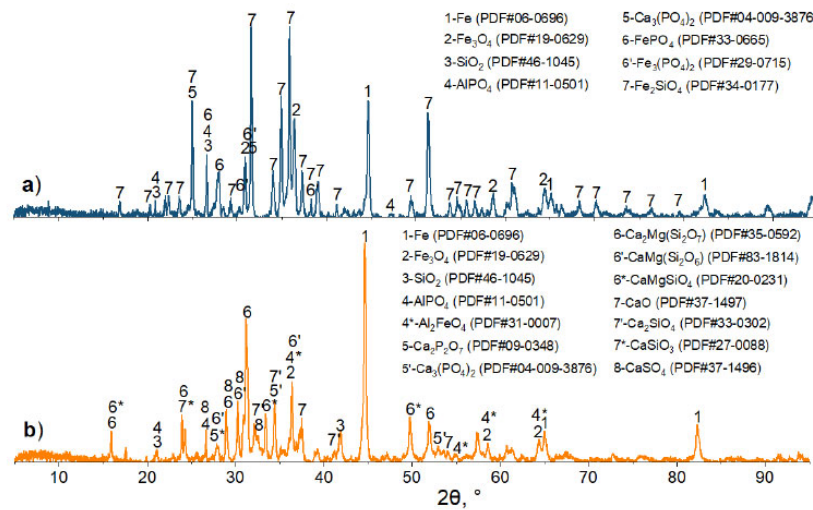


**Fig. (6).** Diffraction patterns of ore samples without (a) and with (b) CaO after reduction roasting with carbon monoxide at 1000°C and a holding time of three hours.

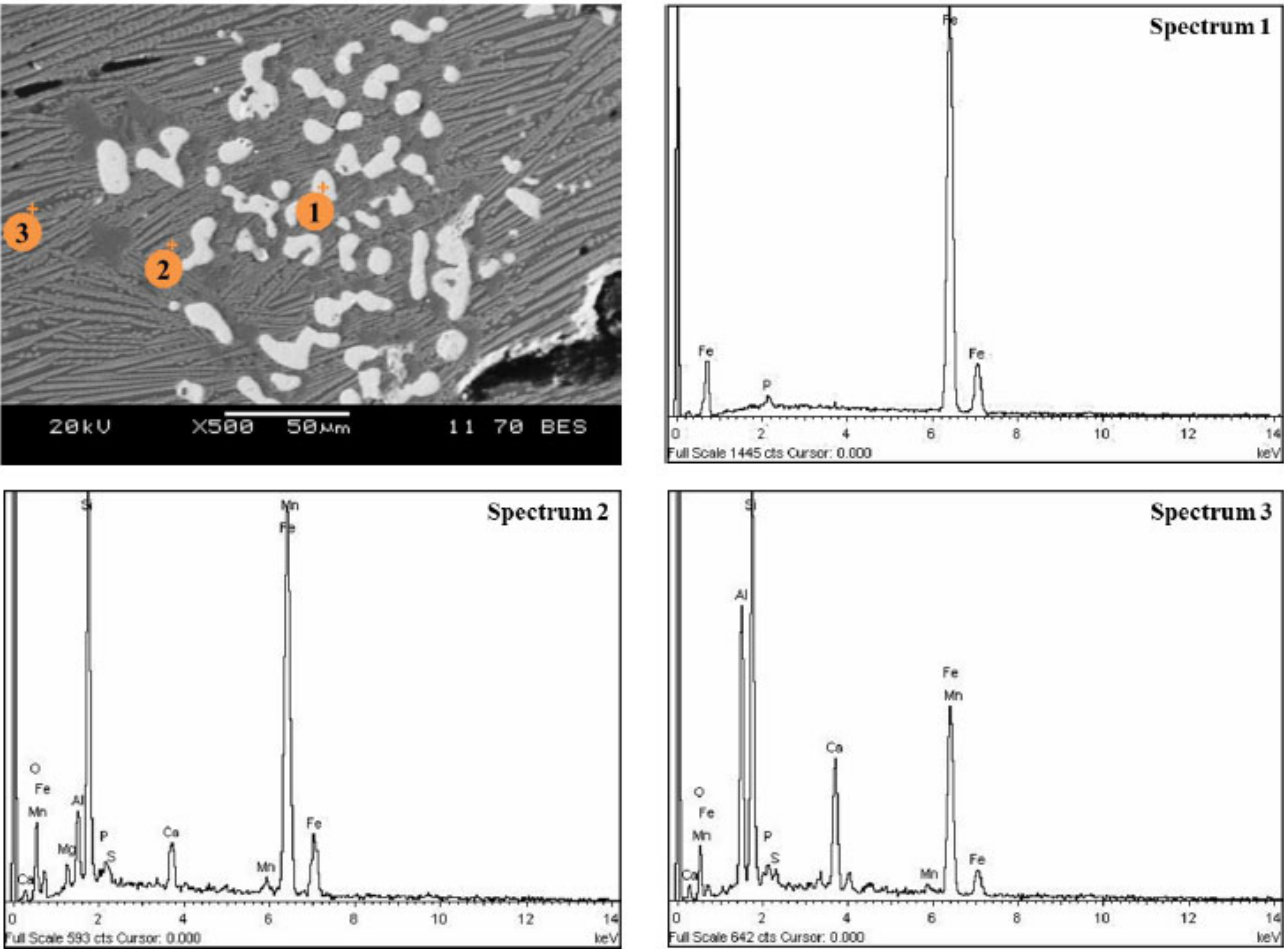


**Fig. (7).** Analysis points and composition of the metal and oxide phase of the smelt after smelting of the non-fluxed product metallized with carbon monoxide.

**Table 2.** The content of elements based on the results of the sample analysis after reduction roasting with carbon monoxide at 1000°C and a holding time of three hours, at. %.

Spectrum	O	Mg	Al	Si	P	S	Ca	Mn	Fe
Spectrum 1	0.0	0.0	0.0	0.0	0.0	0.0	0.0	0.0	100.0
Spectrum 2	12.8	1.1	10.3	15.1	1.8	0.9	9.7	2.0	46.1
Spectrum 3	0.0	0.0	0.0	0.0	0.0	0.0	0.0	0.0	100.0
Spectrum 4	37.9	0.0	17.4	10.7	3.0	0.1	26.6	0.2	4.3

**Table 3.** Composition of metal and slag (wt.%) after the top-and-bottom smelting of the non-fluxed metallized product in CO.

Spectrum	O	Mg	Al	Si	P	S	Ca	Mn	Fe
Spectrum 1	0.0	0.0	0.0	0.0	0.1	0.0	0.0	0.0	99.9
Spectrum 2	14.6	1.7	3.8	18.8	0.4	0.1	2.5	1.1	56.8
Spectrum 3	17.1	0.0	14.7	22.5	0.9	1.3	9.0	0.8	33.6

A piece of metal and separate slag were obtained during the liquid-phase separation of metallized samples with pre-roasting with the addition of lime (Fig. 8).

Table 4 shows the composition of metal and slag after the liquid-phase separation of the reduced oolitic ore samples roasted with the addition of lime. It shows that phosphorus-free metal (iron) and slag with a phosphorus content (0.3 wt.%) were obtained after the separation of the reduction roasting products. The mechanism of phosphorus stabilization with CaO addition is consistent with thermodynamic calculations reported in the literature. In particular, the study [28] shows that an

increase in slag basicity promotes the formation of stable calcium phosphates ( $\text{Ca}_3(\text{PO}_4)_2$ ), reduces phosphorus activity, and suppresses its reduction into the metallic phase. This thermodynamic behavior is in good agreement with the experimental results obtained in the present study.

The 750-fold magnification of the metal on an electron microscope (Fig. 9) can be used to observe inclusions in the form of iron sulfides (spectrum 1) and a separate phase of iron without phosphorus and sulfur (spectrum 2). The quantitative analysis of these phases is presented in Table 5.

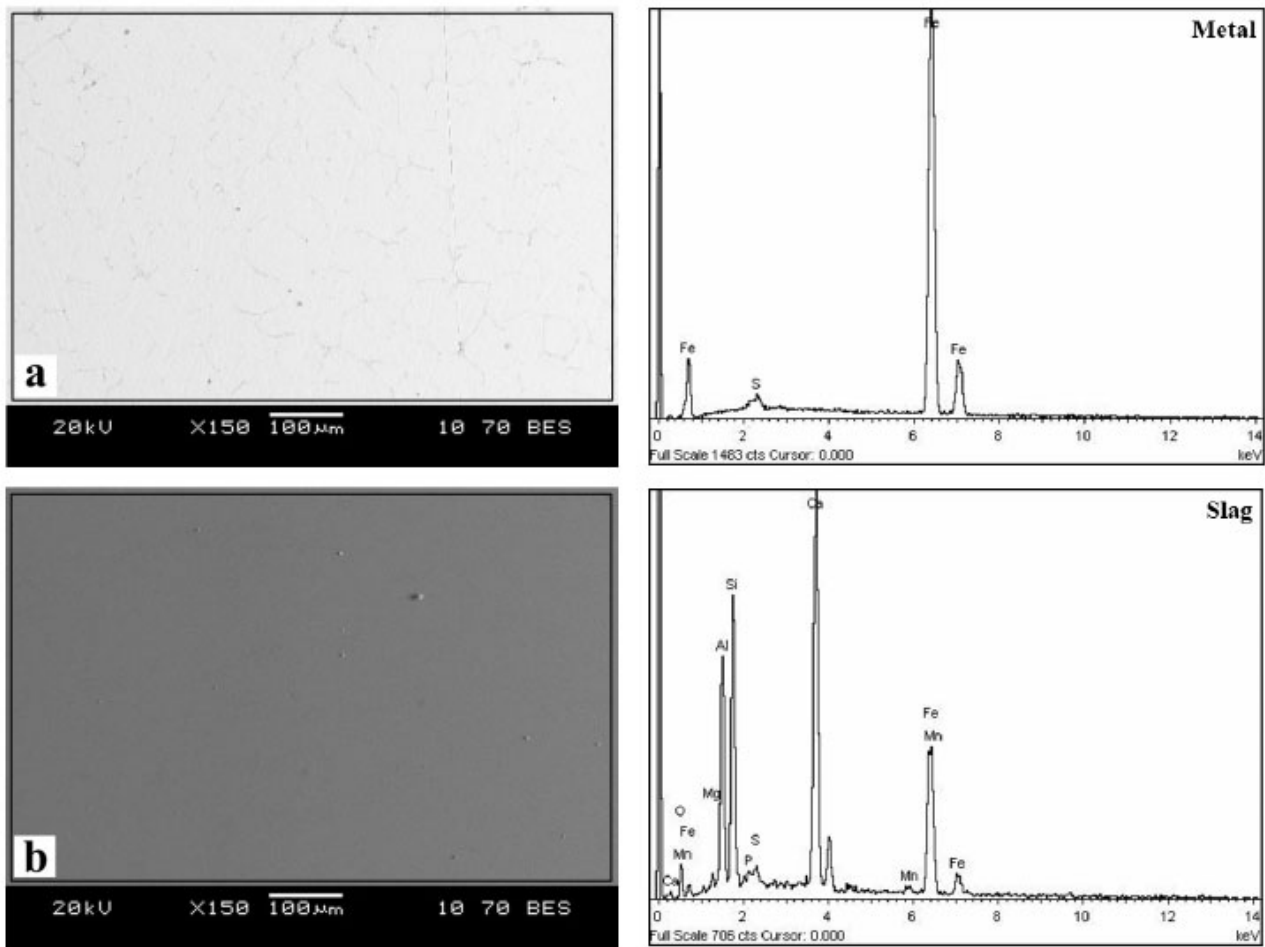


**Fig. (8).** Analysis area and composition of metal (a) and slag (b) after smelting of the fluxed product metallized with carbon monoxide.

**Table 4.** Metal and slag composition (wt.%) after the top-and-bottom smelting of the fluxed product metallized with carbon monoxide.

Section	O	Mg	Al	Si	P	S	Ca	Mn	Fe
Metal (a)	0.0	0.0	0.0	0.0	0.0	0.9	0.0	0.0	99.1
Slag (b)	16.7	0.9	11.6	15.2	0.3	0.7	26.4	1.0	27.2

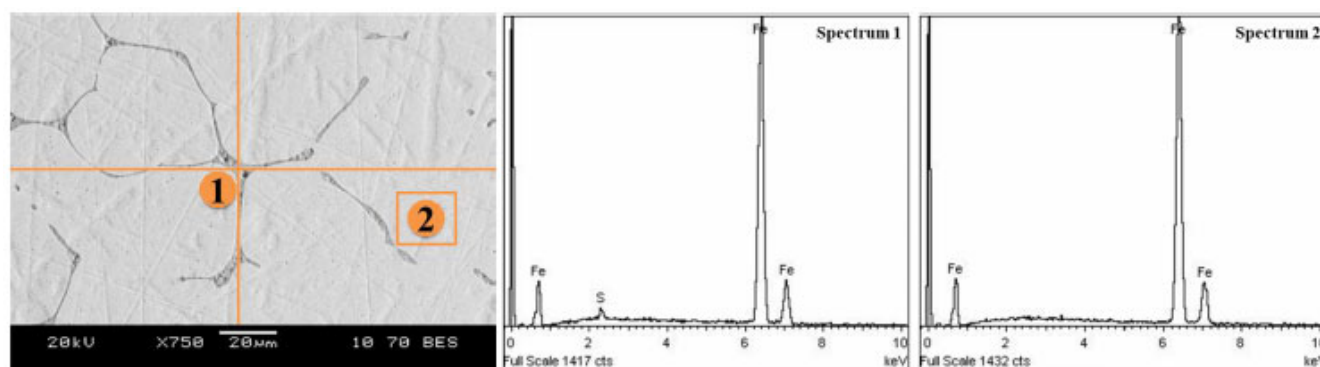


**Fig. (9).** Metal after smelting the fluxed product metallized with carbon monoxide.

**Table 5.** Metal composition (wt.%) after the top-and-bottom smelting of the fluxed product metallized with carbon monoxide.

Spectrum	O	Mg	Al	Si	P	S	Ca	Mn	Fe
Spectrum 1	0.0	0.0	0.0	0.0	0.0	32.6	0.0	0.0	67.4
Spectrum 2	0.0	0.0	0.0	0.0	0.0	0.0	0.0	0.0	100.0

## CONCLUSION

Thus, we demonstrated the possibility of the dephosphorization of high-phosphorous iron ore by preliminary addition of CaO and oxidative roasting with the subsequent solid-phase reduction and liquid-phase separation of the metallization product to obtain low-phosphorus metal and high-phosphorus slag. The following conclusions can be drawn from the results of the experiments:

- [1] The oxidative roasting of the base oolitic ore with the addition of CaO, which brings the basicity to 2.0, leads to the decomposition of iron phosphate  $\text{Fe}_2\text{PO}_4$  and the formation of new calcium phosphates  $\text{Ca}_4\text{P}_2\text{O}_9$  and  $\text{Ca}_2\text{P}_2\text{O}_7$ .
- [2] An increase in basicity prevents the formation of fayalite  $\text{Fe}_2\text{SiO}_4$ , which complicates the reduction of iron in the solid phase. After reduction with carbon monoxide at a basicity of 2.0, the degree of iron reduction increases, while phosphorus is not reduced and remains in the oxide phase in the form of aluminum and calcium phosphates.
- [3] During the liquid-phase separation of fluxed metallized samples, we can prevent the conversion of phosphorus into metal and obtain low-phosphorus metal and high-phosphorus slag.
- [4] Further research is needed for scale-up and optimization of process parameters.

## LIMITATIONS OF THE STUDY

This study was conducted at the laboratory scale, and the results may not fully reflect the behavior of industrial-scale processing of high-phosphorus ores. Thermodynamic modeling (e.g., using FactSage) was not performed;

conclusions on phase transformations were based on XRD data and published literature. EDS analysis was limited to point measurements and does not provide complete information on phase homogeneity. Parameters such as reduction time, CO concentration, and pressure were not systematically varied and require further investigation.

## AUTHORS' CONTRIBUTIONS

The authors confirm their contribution to the paper as follows: study conception and design: B.S., G.A.; data collection: N.K.; analysis and interpretation of results: B.S., N.K.; draft manuscript: B.S. All authors reviewed the results and approved the final version of the manuscript.

## LIST OF ABBREVIATIONS

EDS = Energy Dispersive Spectroscopy  
XRD = X-ray Diffraction

## CONSENT FOR PUBLICATION

Not applicable.

## AVAILABILITY OF DATA AND MATERIALS

The data and supportive information are available within the article.

## FUNDING

None.

## CONFLICT OF INTEREST

The authors declare no conflict of interest financial or otherwise.

## ACKNOWLEDGEMENTS

Declared none.



## REFERENCES

- [1] K.I. Smirnov, P.A. Gamov, and V.E. Roshchin, "Distribution of solid-phase reduction of iron in a layer of ilmenite concentrate", *Ferrous Metallurgy.*, vol. 63, no. 2, pp. 116-121, 2020. [<http://dx.doi.org/10.17073/0368-0797-2020-2-116-121>]
- [2] K.I. Smirnov, P.A. Gamov, V.S. Samolin, and V.E. Roshchin, "Selective reduction of iron from ilmenite concentrate", *Chernye Met.*, vol. 7, pp. 19-23, 2024. [<http://dx.doi.org/10.17580/chm.2024.07.03>]
- [3] S.P. Salikhov, A.V. Roshchin, and V.E. Roshchin, "Theoretical aspects of pyrometallurgical processing of sideroplesite ore", *Chernye Metall.*, no. 8, pp. 13-18, 2018.
- [4] N. Kosdauletov, "Determining the conditions for selective iron recovery by iron-manganese ore reduction", *Steel Transl.*, vol. 50, no. 12, pp. 870-876, 2020. [<http://dx.doi.org/10.3103/S09677091220120050>]
- [5] M.I. Pownceby, "Characterisation of phosphorus and other impurities in goethite-rich iron ores-Possible P incorporation mechanisms", *Miner. Eng.*, vol. 143, p. 106022, 2019. [<http://dx.doi.org/10.1016/j.mineng.2019.106022>]
- [6] Y. Champetier, E. Hamdadou, and M. Hamdadou, "Examples of biogenic support of mineralization in two oolitic iron ores—Lorraine (France) and Gara Djebilet (Algeria)", *Sediment. Geol.*, vol. 51, no. 3-4, pp. 249-255, 1987. [[http://dx.doi.org/10.1016/0037-0738\(87\)90050-9](http://dx.doi.org/10.1016/0037-0738(87)90050-9)]
- [7] E. Donskoi, S.P. Suthers, and M.I. Pownceby, "Ultrasonic treatment of high phosphorus Australian iron ore fines", *Miner. Eng.*, vol. 189, p. 107914, 2022. [<http://dx.doi.org/10.1016/j.mineng.2022.107914>]
- [8] Z. Zhang, and H. Tong, "Spatio-temporal distribution and tectonic settings of the major iron deposits in China: An overview", *Ore Geol. Rev.*, vol. 57, pp. 247-263, 2014. [<http://dx.doi.org/10.1016/j.oregeorev.2013.08.021>]
- [9] S.U. Ofogebu, "Characterization studies on Agbaja iron ore: A high-phosphorus content ore. SN", *Appl. Sci.*, vol. 1, no. 3, 2019. [<http://dx.doi.org/10.1007/s42452-019-0218-9>]
- [10] F. L. C. d'Orey, "The detrital origin of the Moncorvo Ordovician ironstones", *Ciênc. Terra Earth Sci. J.*, vol. 13, 1999.
- [11] M.M. Abro, A.G. Pathan, and A.H. Mallah, "Liberation of oolitic hematite grains from iron ore, Dilband Mines Pakistan. Mehran University Research", *J. Eng. Technol.*, vol. 30, no. 2, pp. 329-338, 2011.
- [12] H. Tang, Z. Guo, and Z. Zhao, "Phosphorus removal of high phosphorus iron ore by gas-based reduction and melt separation", *J. Iron Steel Res. Int.*, vol. 17, no. 9, pp. 1-6, 2010. [[http://dx.doi.org/10.1016/S1006-706X\(10\)60133-1](http://dx.doi.org/10.1016/S1006-706X(10)60133-1)]
- [13] W. Xia, Z. Ren, and Y. Gao, "Removal of phosphorus from high phosphorus iron ores by selective HCl leaching method", *J. Iron Steel Res. Int.*, vol. 18, no. 5, pp. 1-4, 2011. [[http://dx.doi.org/10.1016/S1006-706X\(11\)60055-1](http://dx.doi.org/10.1016/S1006-706X(11)60055-1)]
- [14] A. A. Babenko, and L. A. Smirnov, "Theory and technology of smelting phosphorous cast irons in BOF",
- [15] H.H. Wang, and G.Q. Li, "Dephosphorization of high phosphorus oolitic hematite by acid leaching and the leaching kinetics", *Hydrometallurgy*, vol. 171, pp. 61-68, 2017. [[http://dx.doi.org/10.1016/S1006-706X\(11\)60055-1](http://dx.doi.org/10.1016/S1006-706X(11)60055-1)]
- [16] T.A. Oliinyk, and L V Sklyar, "Development of dephosphorization technology for iron ores with high phosphorus content", *IOP Conf. Ser.: Earth Environ. Sci.*, vol. 1415, no. 1, p. 012063, 2024. [<http://dx.doi.org/10.1088/1755-1315/1415/1/012063>]
- [17] W. Yu, and T. S., "The function of Ca(OH)<sub>2</sub> and Na<sub>2</sub>CO<sub>3</sub> as additive on the reduction of high-phosphorus oolitic hematite-coal mixed pellets", *ISIJ Int.*, vol. 53, no. 3, pp. 427-433, 2013. [<http://dx.doi.org/10.2355/isijinternational.53.427>]
- [18] Hongda Xu, Tichang Sun, Shichao Wu, Xiaoxiao Lian, Wenli Han, and Zongyi Deng, "Research progress on the effects of reducing agents and dephosphorization agents on direct reduction-magnetic separation of high phosphorus oolitic hematite", *Multipurp. Util. Miner. Resour.*, vol. 45, no. 2, pp. 176-184, 2024. [<http://dx.doi.org/10.3969/j.issn.1000-6532.2024.02.029>]
- [19] G. Ji, and Xiao. C., "Direct reduction of high-phosphorus oolitic hematite: Quantifying phosphorus migration and recovery", *Metall. Mater. Trans.*, vol. 55, no. 5, pp. 3107-3121, 2024. [<http://dx.doi.org/10.1007/s11663-024-03165-4>]
- [20] Y.S. Sun, Y.X. Han, P. Gao, Z.H. Wang, and D.Z. Ren, "Recovery of iron from high phosphorus oolitic iron ore using coal-based reduction followed by magnetic separation", *Int. J. Miner. Metall. Mater.*, vol. 20, no. 5, pp. 411-419, 2013. [<http://dx.doi.org/10.1007/s12613-013-0744-1>]
- [21] P. Delvasto, and A. Ballester, "Mobilization of phosphorus from iron ore by the bacterium *Burkholderia caribensis* FeGL03", *Miner. Eng.*, vol. 22, no. 1, pp. 1-9, 2009. [<http://dx.doi.org/10.1016/j.mineng.2008.03.001>]
- [22] J. Pan, and Shenghu Lu, "A new route to upgrading the high-phosphorus oolitic hematite ore by sodium magnetization roasting-magnetic separation-acid and alkaline leaching process", *Minerals*, vol. 12, no. 5, p. 568, 2022. [<http://dx.doi.org/10.3390/min12050568>]
- [23] V.G. Karelin, L.A. Zainulin, and A.Y. Epishin, "Combined pyrohydrometallurgical technology of dephosphorizing brown ironstone of Lisakovsky deposit", *Bull. Sci. Tech. Econ. Inf.*, no. 2, pp. 10-15, 2015.
- [24] V.G. Karelin, L.A. Zainulin, and A.Y. Epishin, "Features of pyrohydrometallurgical technology of dephosphorizing brown ironstone of Lisakovsky deposit", *Steel*, no. 3, pp. 8-11, 2015.
- [25] B. Suleimen, S.P. Salikhov, and V.Y. Roshchin, "Study of the iron ores of the Ayat deposit of the oolite type", *Min. Inf. Anal. Bull.*, vol. 10, no. 10-1, pp. 50-58, 2022. [[http://dx.doi.org/10.25018/0236\\_1493\\_2022\\_101\\_0\\_50](http://dx.doi.org/10.25018/0236_1493_2022_101_0_50)]
- [26] S.P. Salikhov, B. Suleimen, and V.E. Roshchin, "Selective reduction of iron and phosphorus from oolite ore", *Ferrous Metallurgy.*, vol. 63, no. 7, pp. 560-567, 2020. [<http://dx.doi.org/10.17073/0368-0797-2020-7-560-567>]
- [27] B. Suleimen, S.P. Salikhov, F.S. Sharipov, and V.E. Roshchin, "Selective solid-phase reduction of iron in phosphorous oolite ores", *Izv. Ferrous Met.*, vol. 66, no. 4, pp. 479-484, 2023. [<http://dx.doi.org/10.17073/0368-0797-2023-4-479-484>]
- [28] C. Chen, L. Zhang, and J. Lehmann, "Thermodynamic modelling of phosphorus in steelmaking slags", *High-Temp. Mater. Process.*, vol. 32, no. 3, p. 237, 2013. [<http://dx.doi.org/10.1515/htmp-2012-0129>]

**DISCLAIMER:** The above article has been published, as is, ahead-of-print, to provide early visibility but is not the final version. Major publication processes like copyediting, proofing, typesetting and further review are still to be done and may lead to changes in the final published version, if it is eventually published. All legal disclaimers that apply to the final published article also apply to this ahead-of-print version.